AD-A126 429 THE FATIGUE OF POWDER METALLURGY ALLOYS(U) CONNECTICUT 1/
UNIV STORRS DEPT OF METALLURGY A J MCEVILY 17 JAN 83
AFOSR-TR-83-0128 AFOSR-81-0046

UNCLASSIFIED F/G 11/6 NL

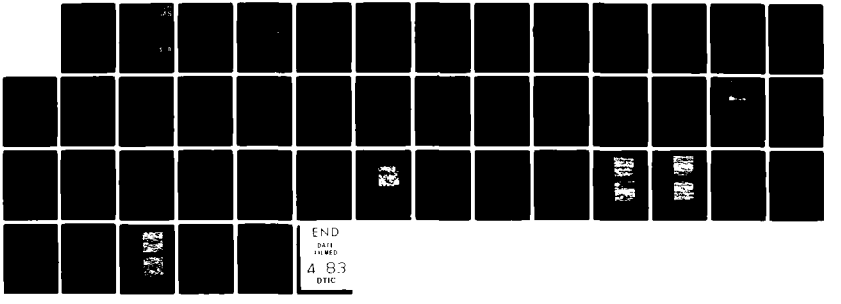

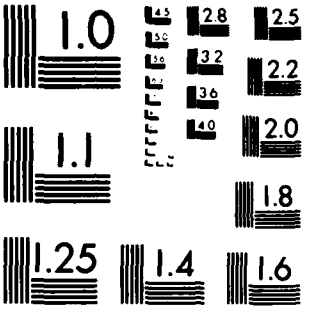

IMS

INSTITUTE OF MATERIALS SCIENCE

Annual Report
on
The Fatigue of Powder Metallurgy Alloys
U.S. Air Force Grant No. AFOSR 81-0046

Covering Period
1 December 1981 to 30 November 1982

Submitted by

A. J. McEvily

THE UNIVERSITY OF CONNECTICUT
Storrs · Connecticut

Annual Report
on
The Fatigue of Powder Metallurgy Alloys
U.S. Air Force Grant No. AFOSR 81-0046

Covering Period
1 December 1981 to 30 November 1982

Submitted by

A. J. McEvily

UNCLASSIFIED

SECURITY CLASSIFICATION OF THIS PAGE (When Data Entered)

REPORT DOCUMENTATION PAGE		READ INSTRUCTIONS BEFORE COMPLETING FORM
1. REPORT NUMBER AFOSR-TR- 83-0128	2. GOVT ACCESSION NO. AD-A126 429	3. RECIPIENT'S CATALOG NUMBER
4. TITLE (and Subtitle) THE FATIGUE OF POWDER METALLURGY ALLOYS		5. TYPE OF REPORT & PERIOD COVERED Scientific ----- Annual 12/1/81 - 11/30/82
		6. PERFORMING ORG. REPORT NUMBER
7. AUTHOR(s) A. J. McEvily, Jr		8. CONTRACT OR GRANT NUMBER(s) AFOSR-81-0046
9. PERFORMING ORGANIZATION NAME AND ADDRESS University of Connecticut Metallurgy Dept. Storrs, CT 06268		10. PROGRAM ELEMENT, PROJECT, TASK AREA & WORK UNIT NUMBERS 61102F 2306/A1
11. CONTROLLING OFFICE NAME AND ADDRESS Air Force Office of Scientific Research Bolling AFB, Building 410 Washington, D.C. 20332		12. REPORT DATE January 17, 1983
		13. NUMBER OF PAGES 41
14. MONITORING AGENCY NAME & ADDRESS (if different from Controlling Office)		15. SECURITY CLASS. (of this report) Unclassified
		15a. DECLASSIFICATION DOWNGRADING SCHEDULE

16. DISTRIBUTION STATEMENT (of this Report)

This document has been approved for public release [redacted]; its distribution is unlimited.

17. DISTRIBUTION STATEMENT (of the abstract entered in Block 20, if different from Report)

18. SUPPLEMENTARY NOTES

19. KEY WORDS (Continue on reverse side if necessary and identify by block number)

High Strength Aluminum Powder Metallurgy Alloys
Fatigue Crack Propagation
Fatigue Threshold
Crack Closure
Corrosion Fatigue

20. ABSTRACT (Continue on reverse side if necessary and identify by block number)

Fatigue crack growth in the powder metallurgy alloys X7090-T6, X7091-T7E69, and IN 9021-T4 has been studied as a function of R ratio in air. Additional tests in a 3-1/2% NaCl environment have also been made. S/N properties of X7090-T6 and X7091-T7E69 have been determined. Fatigue data of 7075-T6, an ingot metallurgy product, have been obtained for comparison. Attention has focused on the effect of microstructure and crack closure in the near threshold region. Of particular interest was the lack of detectable closure in the IN9021 alloy even at threshold. This alloy had the lowest threshold of the various alloys tested.

(continued)

DD FORM 1 JAN 73 1473 EDITION OF 1 NOV 65 IS OBSOLETE

UNCLASSIFIED

SECURITY CLASSIFICATION OF THIS PAGE (When Data Entered)

In one series of tests on X7090-T6 material was removed from behind crack tip in order to understand better the influence of material remote from the crack tip on the closure process. A relatively small effect was found, an indication that closure principally results from near tip contacts. The effect of a 3-1/2% NaCl environment was found to depend on the alloy. For 7075-T76 the threshold level was increased due to the presence of corrosion products which increased closure levels. For the T-L orientation of X7090-T6 and X7091-T7E69, the threshold levels decreased, an indication that possible beneficial effects of corrosion products on closure were offset by the aggressive characteristics of the environment.

Annual Report

on

The Fatigue of Powder Metallurgy Alloys

U. S. Air Force Grant No. AFOSR 81-0046

Covering Period

1 December 1981 to 30 November 1982

Submitted to

The Air Force Office of Scientific Research

AFOSR/NE

Bolling AFB

Washington, DC 20332

Attn: Dr. Alan H. Rosenstein
Program Manager

Submitted by

Professor A. J. McEvily, Jr.
Metallurgy Department U-136
University of Connecticut
Storrs, Connecticut 06268
(203) 486-2941

January 1983

ABSTRACT

Fatigue crack growth in the powder metallurgy alloys X7090-T6, X7091-T7E69, and IN 9021-T4 has been studied as a function of R ratio in air. Additional tests in a 3-1/2% NaCl environment have also been made. S/N properties of X7090-T6 and X7091-T7E69 have been determined. Fatigue data of 7075-T6, an ingot metallurgy product, have been obtained for comparison. Attention has focused on the effect of microstructure and crack closure in the near threshold region. Of particular interest was the lack of detectable closure in the IN9021 alloy even at threshold. This alloy had the lowest threshold of the various alloys tested. In one series of tests X7090-T6 material was removed from behind crack tip in order to understand better the influence of material remote from the crack tip on the closure process. A relatively small effect was found, an indication that closure principally results from near tip contacts. The effect of a 3-1/2 NaCl environment was found to depend on the alloy. For 7075-T76 the threshold level was increased due to the presence of corrosion products which increased closure levels. For the T-L orientation of X7090-T6 and X7091-T7E69, the threshold levels decreased, an indication that possible beneficial effects of corrosion products on closure were offset by the aggressive characteristics of the environment.

INTRODUCTION

This report covers the second year of a program of research aimed at improving our understanding of fatigue processes in powder metallurgy (P/M) alloys of interest in structural applications. During this period attention has been focused on the fatigue crack growth characteristics of three P/M aluminum alloys, X7090-T6, X7091-T7E69 and IN9021-T4, a mechanically alloyed product. Additional tests of the ingot metallurgy (I/M) alloy 7075-T76 have been carried out for purposes of comparison. The results of tests in air as a function of mean stress level, and in sodium chloride environments will be described. Particular attention has been given to the near-threshold region and the role of crack-closure therein. In addition the S/N properties have been obtained to X7090-T6, X7091-T7E69, and 7075-T76.

MATERIALS AND EXPERIMENTS

The following alloys were obtained in extruded form from ALCOA via the Lockheed-California Company:

P/M X7090-T6

P/M X7091-T7E69

I/M 7075-T6

The mechanically alloyed P/M product was obtained from Novamet as a forged plate.

The nominal chemical compositions for these materials are given in Table I. The tensile properties as determined in our laboratory are given in Table II. The microstructures of the three P/M alloys are shown in Fig. 1 for comparison. Additional microstructural views are shown in the previous annual report.

The S/N fatigue tests were conducted on hour-glass shaped specimens under fully reversed axial load test conditions (R = -1). The tests were carried out at 30 Hz at 20°C and a relative humidity of 50%. A sinusoidal wave form was employed. Specimen surfaces were polished longitudinally with 1 μm diamond paste prior to testing. The specimen axis was in the direction of extrusion.

The specimens for fatigue crack growth tests were 6.3 mm thick of the ASTM compact type with an effective width, W, of 57.2 mm and a half-height, H, of 34.4 mm (H/W = 0.6). The specimens from the ALCOA products were machined from 1.5-inch thick sections in the T-L orientation. The specimens from the Novamet product were machined from a 1-inch thick section. Because of the extent of material removed during machining any possible residual stress effects on fatigue behavior is thought to be minimal. In determining the rate of fatigue crack growth as well as the threshold level a ΔK-decreasing test was employed. In this procedure loads were reduced by 10% or less and the crack was allowed to grow a distance corresponding to at least five times the monotonic plane stress plastic zone of the previous loading for each load decrement. ΔK_{TH} was determined as the stress intensity factor, ΔK at which no crack growth was observed for at least 2×10^6 cycles. The crack opening characteristics were also examined using the modified elastic compliance method in which an elastic compliance was electronically subtracted from the total crack opening displacement (COD) signal to increase sensitivity.

RESULTS AND DISCUSSIONS

I. High Cycle Fatigue Properties (S-N)

High cycle fatigue properties (S-N) for P/M X7090-T6 and X7091-T7E69 alloys as well as an I/M 7075 T76 examined. The results are presented in Fig. 2. It is noted that both of the P/M alloys exhibit superior fatigue resistance as compared to the I/M 7075 alloy. This result may reflect the higher yield strength of the P/M aluminum alloys as compared to the I/M aluminum alloy. The results of high cycle fatigue tests together with tensile properties are summarized in Table III.

II. Near-Threshold Fatigue Crack Growth in 3-1/2% NaCl Solution

Near-threshold fatigue crack growth in 3-1/2% NaCl solution was studied for the P/M X7090-T6 and X7091-T7E69 alloys as well as the I/M 7075-T76 alloy in the T-L orientation. All tests were conducted at R = 0.05.

The results of crack growth tests in 3-1/2 NaCl solution together with results in air are presented in Figs. 3-5. Also shown in Figs. 6-8 are the results of crack opening load measurements. In the intermediate region, the crack growth rates in NaCl solution are higher than those in air at a given ΔK level for all alloys. In the near-threshold region growth rates in the NaCl solution for the I/M 7075 alloy were slower than in air but faster for the P/M X7090 and X7091 alloys. As shown in Figs. 6-8 all alloys showed that in the NaCl solution the crack closure level rapidly increased as the stress intensity approached ΔK_{TH}. Fractographic analyses revealed that a great extent of corrosion debris had built up between the mating fracture surfaces in the NaCl environment. A typical example of corrosion products observed on the fracture

surface of the X7091 alloy is shown in Fig. 9. Since these corrosion products significantly reduce the effective crack tip opening displacement (1,2), the observed increase in closure level in the NaCl environment is strongly associated with thick corrosion products. In all cases thickening corrosion products significantly contributed to the arrest of the crack at threshold. However, a process for thickening corrosion products appears to vary with the type of alloy. In order to show this variation in thickening process of corrosion products, the results of crack opening load measurements for K-decreasing tests for all three alloys shown in Figs. 6-8 are replotted in Fig. 10. This figure clearly indicates that the crack closure levels for the I/M 7075 are higher than those for the P/M alloys at a given ΔK level. Since the closure level in corrosive environments such as the present NaCl solution is strongly associated with thickness of corrosion products, the result seen in Fig. 10 indicates that corrosion products developed in the I/M 7075 alloy are easier to thicken as compared to the P/M products.

III. Load Ratio Effect on the Near-Threshold Fatigue Crack Growth

The effect of load ratio on the near-threshold fatigue crack growth was examined for the P/M X7090T6 alloy. Fatigue crack growth tests were conducted on the 6.3 mm thick compact type specimens machined in the T-L orientation. Fig. 11 shows the da/dN vs. ΔK plots obtained at three different R ratios, 0.05, 0.5 and 0.8. The influence of the load ratio on the threshold level and fatigue crack growth rates is apparent, i.e., as the load ratio increases growth rates for a given ΔK level increase and the threshold level decreases. The results of crack opening load

measurements are presented in Fig. 12. This figure indicates the significant load ratio effect on crack closure characteristics of this P/M aluminum alloy. At R = 0.05 crack closure levels were high in the near-threshold region and decreased to a much lower level as ΔK increased. The crack closure level is much lower at R = 0.5 as compared to that at R = 0.05. Furthermore, no crack closure was observed at R = 0.8. At R = 0.05, the significant fractographic features in the near-threshold region are the shear facets, indicating that the shear mode crack growth is dominant in the near-threshold region (Fig. 13(a)). The fracture appearance at the threshold level shown in Fig. 13(b) was smooth. This smooth fracture surface was due to extensive fretting action taking place behind the crack tip. As shown in Fig. 14(a) shear facets were observed at R = 0.5. However, these shear facets formed only near to the threshold level, approximately below a ΔK of 2 MPa$\sqrt{m}$. The shear facets at R = 0.5 are smaller and more sharply defined than those at R = 0.05. At R = 0.8 where no crack closure was obtained, shear facets were observed only very near to the threshold level, approximately less than 1.3 MPa$\sqrt{m}$. As shown in Fig. 14(b) the shear facets observed at R = 0.8 are very sharply defined, indicating that the extensive fretting action which occurs at R = 0.05 is absent. The present study reveals that a combination of Mode II and Mode I crack growth (3) took place in the near-threshold region at all R ratios. However, increasing the load ratio lowers the onset of the Mode II crack process. As a result the presence of shear facets appears to be restricted to a much narrower ΔK range at the higher load ratios. A variation of load ratios considerably alters fracture appearance in the near-threshold region, particularly the sharpness of shear facets.

The high crack tip closure force at R = 0.05 results in considerable fretting action between the mating fracture surfaces. As a result the fracture surface becomes smooth. Increasing load ratio decreases the crack closure force, resulting in less fretting action. Therefore the higher the load ratio the more sharply defined shear facets become.

An overall representation of the effect of R ratio on ΔK_{TH} is shown in Fig. 15. For positive R ratios crack closure is most pronounced near R = 0. As the R ratio increases the extent of closure (and the role of Mode II) decreases. At R ratios above 0.6 the full ΔK range is effective in propagating a crack just above the threshold. Note that as R ratio approaches 1.0 the fracture toughness of the material places an upper limit on the value of Kmax. In the R regime close to R = 1.0 the value of Kmax is fixed by K_c and the value of Kmin by the relation $K_{min} = K_c R$.

For values of R in the negative region, if the compressive load can serve to further close the crack, the value of Kmax at threshold will decrease and there is some evidence for this (7). On the other hand if the crack is closed at R = 0, then the value of Kmax may not decrease on going into the negative R region. As negative R ratio increases, the compressive yield strength of the material places a lower limit on the value of Kmin. Further work at negative R radios is needed to understand this behavior more thoroughly.

IV. Crack Closure Characteristics in the Near-Threshold Region

It has been recognized that crack closure levels are high because of a combination of Mode II and Mode I crack growth (3) as well as oxide or corrosion products (1,2). However, Newman (4) recently suggested

based upon his computer analysis of crack closure characteristics that the fatigue thresholds obtained in load reduction schemes artifically develop as a result of the high closure effect due to the residual plastic deformation in the wake of the advancing crack. In the present study the influence of the load-reduction schemes on the rate of fatigue crack growth and the crack opening load characteristics were critically examined with 6.3 mm thick compact type specimens machined from the X7090 alloy in the T-L orientation. In order to examine the influence of the load reduction schemes, the stretched material due to plastic deformation in the wake of the advancing crack was removed by electro-discharge machining. After cutting the K_{op} level was reevaluated and the rate of crack growth was also redetermined at the same ΔK level. Fig. 16 shows the results of the fatigue crack growth test. Also shown in Fig. 17 are the results of crack opening load measurements in terms of K_{op} as a function of ΔK. A threshold level of 2.2 MPa$\sqrt{m}$ was first obtained by a ΔK-decreasing procedure. Then a cut was made to remove the stretched material in the wake of the crack. The length from end of the cut to the crack tip was approximately 0.9 mm. As a result of this cut, the crack which had not grown for 2×10^6 cycles started again and propagated at a growth rate of 1.5×10^{-6} mm/cycle. As shown in Fig. 16, a new threshold developed at ΔK = 2.0 MPa$\sqrt{m}$ in a subsequent ΔK-decreasing test. The corresponding reduction in K_{op} is 0.25 MPa$\sqrt{m}$. Since the cutting removed the contribution to the crack closure from the combination of Mode II and Mode I crack growth in the near-threshold region in addition to the residual plastic deformation, these differences between the two fatigue thresholds and the corresponding K_{op} levels are considered to be very small. It is important to note that the fatigue

threshold can develop without any contribution of the residual stretch in the wake of the advancing crack at least for distances behind the crack tip greater than 0.9 mm. From these results, it is concluded that the near-threshold fatigue crack growth is strongly associated with the Mode II and Mode I crack growth.

V. Near-Threshold Fatigue Crack Growth in a (MA) IN 9021-T4 Alloy

The near-threshold fatigue crack growth of an IN 9021-T4 aluminum alloy is being investigated. This alloy was produced by means of mechanical alloying (MA). The MA process is a unique high energy milling process for producing metal powders (5) and the resultant microstructure contains a uniform, equiaxed fine dispersion of oxygen and carbon particles. It has been reported (6) that this alloy shows excellent mechanical properties as well as a superior resistance to stress-corrosion cracking. The chemical composition and tensile properties of this alloy are shown in Table I and Table II. Fatigue crack growth tests were conducted on 6.3 mm thick compact type specimens machined from a forged plate in the T-L orientation. An example of the microstructure is shown in Fig. 1(c). This micrograph taken with an optical microscope at a magnification of 1000 did not reveal any grains, suggesting a very fine grained microstructure. In fact, we were informed by Novamet, producer of IN 9021-T4 alloy, that the average grain size of this alloy is of the order of 0.2 μm. This grain size is much finer than those of the P/M X7090 and X7091 alloys (approximately 1 μm ~ 10 μm). TEM (Transmission Electron Microscopy) studies to characterize the microstructure of the IN 9021-T4 alloy are planned in the third year of the program.

The rates of fatigue crack growth at R = 0.05 and R = 0.5 are presented in Fig. 18 as a function of ΔK. Fig. 18 also includes results for the 7075 T76 alloy for purposes of comparison. As seen in the figure, at R = 0.05 faster growth rates and a lower threshold level were obtained in the IN 9021 alloy as compared to the 7075 alloy. It is noted that the threshold level of this alloy (ΔK_{TH} = 0.85 MPa$\sqrt{m}$) is lower than those of the P/M X7090 and X7091 alloys (ΔK_{TH} = 2.3 MPa$\sqrt{m}$ for the X7090 alloy, ΔK_{TH} = 2.4 MPa$\sqrt{m}$ for the X7091 alloy) in the same orientation. Although the R = 0.5 test has not been completed, data points in the near-threshold region are also shown in Fig. 18. Fatigue crack growth rates at R = 0.5 as a function of ΔK are similar to those at R = 0.05, indicating that the near-threshold fatigue crack growth of the IN 9021 alloy is independent of load ratio. It is important to note that no detectable crack closure was obtained for both the R = 0.05 and R = 0.5 tests. No influence of load ratio on the near-threshold crack growth associated with no crack closure in the IN 9021 alloy is contrasted with the near-threshold crack growth of the X7090-T6 alloy in which the significant load ratio effect on the near-threshold crack growth behavior was observed as described in Section III of this report. A fractographic study on the fracture surface of the IN 9021 alloy tested at R = 0.05 revealed that the fracture appearance in the near-threshold region is extremely smooth, as shown in Fig. 19. The crack path in the near-threshold region appears to be transgranular. The smooth fracture surface observed in the near-threshold region of the IN 9021 alloy is contrasted by the tortuous very tall crystallographic appearance

obtained. In general for most alloys at low load ratios, closure levels in the near-threshold region are high because of the Mode II and Mode I crack growth. The importance of the Mode II contribution is to develop mismatch of crack faces necessary for high crack closure through a tortuous crack path. However, for a microstructure with very fine grains, the tortuosity is limited and therefore it is difficult for mismatch to occur. From the present fractographic analysis the lack of crack path tortuosity is evident in the IN 9021 alloy.

VI. Comparison of Alloys

Fig. 20 compares the fatigue crack growth behavior in the near-threshold region for the aluminum alloys investigated. IN 9021, which shows an absence of detectable closure exhibits the lowest threshold level. The other three alloys all exhibit high thresholds as well as closure but there is not a one-to-one correspondence between these characteristics, probably because errosion behind the crack tip affects the closure level difference in these alloys. Above the near-threshold region the crack growth rates in the P/M alloys are higher than in the I/M alloy, and this may be associated with lower closure levels of the P/M alloys in this growth rate region as compared to the I/M alloy.

References

1. A. T. Stewart, Engineering Fracture Mechanics, 1980, Vol. 13, p. 463.

2. S. Suresh, G. F. Zamiski and R. O. Ritchie, Metallurgical Trans. A, 1981, Vol. 12A, p. 1435.

3. K. Minakawa and A. J. McEvily, Scripta Metallurgica, 1981, Vol. 15, p. 633.

4. J. C. Newman, AGARD Specialists Meeting on Behavior of Short Cracks in Airframe Components, September, 1982, Toronto, Canada.

5. J. S. Benjamin and R. D. Schelleng, Metallurgical Trans. A, 1981, Vol. 12A, p. 813.

6. D. L. Erich and S. J. Donachie, Metal Progress, 1982, February, p. 22.

7. A. Ohta, M. Kosuge and E. Sasaki, International J. of Fracture, Vol. 14, 1978, p. 251.

Papers Published

A. J. McEvily and K. Minakawa, "Fatigue Crack Growth in the Near-Threshold Region", in Strength of Metals and Alloys, R. C. Gifkins, Ed., Pergamon Press, 1982, Vol. 2, p. 845.

Paper Submitted

A. J. McEvily, "On the Quantitative Analysis of Fatigue Crack Propagation" to be published in ASTM Special Technical Publication.

Paper in Preparation

K. Minakawa, J. C. Newman and A. J. McEvily, "A Critical Study of the Crack Closure Effect on Near-Threshold Fatigue Crack Growth".

Presentations

1. A. J. McEvily, "Fatigue Crack Propagation" seminar at Inco Research and Development Center, Suffern, March, 1982.
2. K. Minakawa, J. A. Ruppen and A. J. McEvily, "On Fatigue Crack Growth in Aluminum and Titanium Alloys in the Near-Threshold Region", ASTM Symposium "Fractography in Failure Analysis of Ceramics and Metals", Philadelphia, April, 1982.
3. A. J. McEvily, "On the Quantitative Analysis of Fatigue Crack Propagation" Symposium on Int. Conf. on Quantitative Measurement of Fatigue Damage, Dearborn, May 1982.
4. A. J. McEvily, "Fatigue Crack Propagation", seminar at NASA Lengley, Hampton, June, 1982.
5. A. J. McEvily and K. Minakawa, "Fatigue Crack Growth in the Near-Threshold Region", 6th Int. Conf. on the Strength of Metals and Alloys, Melbourne, August, 1982.
6. S. Z. Liu and A. J. McEvily, "Effect of Variable Amplitude Loading on the Fatigue Life of Titanium", 1982 TMS-AIME Fall Meeting, St. Louis, October, 1982.
7. A. J. McEvily, "Fatigue Crack Propagation", ASM Rhode Island Chapter Meeting, Providence, November, 1982.

Personnel

Principal Investigator:	A. J. McEvily, Professor
Associate Investigator:	K. Minakawa, Asst. Professor
Research Technician:	R. Shover
Ph.D. Candidate:	J. A. Ruppen
Ph.D. Recipient:	C. Hoffman
M.S. Candidate:	G. Levan
M.S. Recipients:	G. Gikas
	J. Bunch

Figure Captions

Fig. 1 Microstructures taken from the longitudinal sections of P/M aluminum alloys, (a) X7090-T6, (b) X7091-T7E69, (c) 1N9021-T4.

Fig. 2 Number of cycles to failure vs. maximum stress for aluminum alloys tested at R = -1.

Fig. 3 Fatigue crack growth rates of X7090 aluminum alloy tested at R = 0.05 in 3.5 pct. NaCl solution.

Fig. 4 Fatigue crack growth rates of X7091 aluminum alloy tested at R = 0.05 in 3.5 pct. NaCl solution.

Fig. 5 Fatigue crack growth rates of 7075 aluminum alloy tested at R = 0.05 in 3.5 pct. NaCl solution.

Fig. 6 Results of crack opening load measurements for X7090 aluminum alloy tested in 3.5 pct. NaCl solution.

Fig. 7 Results of crack opening load measurements for X7091 aluminum alloy tested in 3.5 pct. NaCl solution.

Fig. 8 Results of crack opening load measurements for 7075 aluminum alloy tested in 3.5 pct. NaCl solution.

Fig. 9 Fracture surface of X7091 tested at R = 0.05 in 3.5 pct. NaCl solution. Note that corrosion products developed on the fracture surface. Arrow indicates direction of macroscopic crack growth.

Fig. 10 Comparison of closure levels for three types of aluminum alloys tested at R = 0.05 in 3.5 pct. NaCl solution. Data points were taken from only K-decreasing tests for all alloys.

Fig. 11 Fatigue crack growth rates of X7090 aluminum alloy tested at three R ratios.

Fig. 12 Results of crack opening load measurements for X7090 aluminum alloy at three R ratios. Note that no closure was observed at R = 0.8.

Fig. 13 Fracture surface of X7090 aluminum alloy tested at R = 0.05. Arrow indicates direction of macroscopic crack growth. (a) 5×10^{-6} mm/cycle, (b) ΔK_{TH}.

Fig. 14 Appearance of fracture surface of X7090 aluminum alloy at ΔK_{TH}. Arrow indicates direction of macroscopic crack growth. (a) R = 0.5, (b) R = 0.8.

Fig. 15 Overall representation of the effect of R ratio on ΔK_{TH}. Solid lines indicate a variation of K level obtained from the present study. Dash lines indicate an expected variation of K level as a function of R. (Assuming that a crack is fully closed at R = 0.)

Fig. 16 Results of the near-threshold fatigue crack growth test for X7090 aluminum alloy. Note that the difference between the two thresholds is only 0.2 MPa$\sqrt{m}$.

Fig. 17 Results of crack opening load measurements for X7090 aluminum alloy. Note that closure characteristics are strongly associated with the Mode II and Mode I crack growth.

Fig. 18 Fatigue crack growth rates of IN 9021 aluminum alloy tested at R = 0.05 and R = 0.5.

Fig. 19 Appearance of fracture surface in the near-threshold region of IN 9021 aluminum alloy tested at R = 0.05. Arrow indicates direction of macroscopic crack growth. (a) 1×10^{-6} mm/cycle, (b) ΔK_{TH}.

Fig. 20 Comparison of fatigue crack growth behavior in the near-threshold region for the aluminum alloys.

Table I Nominal Chemical Compositions (Wt%)

	Cu	Mg	Mn	Si	Fe	Co	Zn	Ti	Cr	C	O
7090 T6	0.60-1.30	2.00-3.00		max 0.12	max 0.15	1.00-1.90	7.30-8.70				
7091 T7E69	1.20-2.00	2.20-3.00		max 0.15	max 0.20	0.20-0.60	6.00-7.00				
7075 T76	1.20-2.00	2.10-2.90	max 0.30	max 0.40	max 0.50		5.10-6.10	max 0.20	0.18-0.28		
N9021 T4	4.00	1.50		0.05	0.20					1.10	0.80

Table II Tensile Properties

	Orientation	σ_{ys}(MPa)	UTS(MPa)	Elongation (%)*
X7090 T6	L	650	683	8.5
	T	580	634	8.2
X7091 T7E69	L	544	593	13
	T	527	580	12
7075 T76	L	471	540	7
	T	420	461	6
1N9021 T4	L	535	600	7.2
	T	523	587	8.3

*25.4 mm gage length

Table III Fatigue Resistance at 10^7 Cycles and Yield Strength

Alloy	Fatigue Resistance at 10^7 Cycles (MPa)	Yield Strength (MPa)*
X7090-T6	276	650
X7091-T7E69	262**	544
7075-T76	235	471

*longitudinal direction

**fatigue resistance for the X7091-T7E69 alloy was determined at 8×10^6 cycles.

(a) (b) (c)

Fig. 1 Microstructures taken from the longitudinal sections of P/M aluminum alloys, (a) X7090-T6, (b) X7091-T7E69, (c) IN9021-T4.

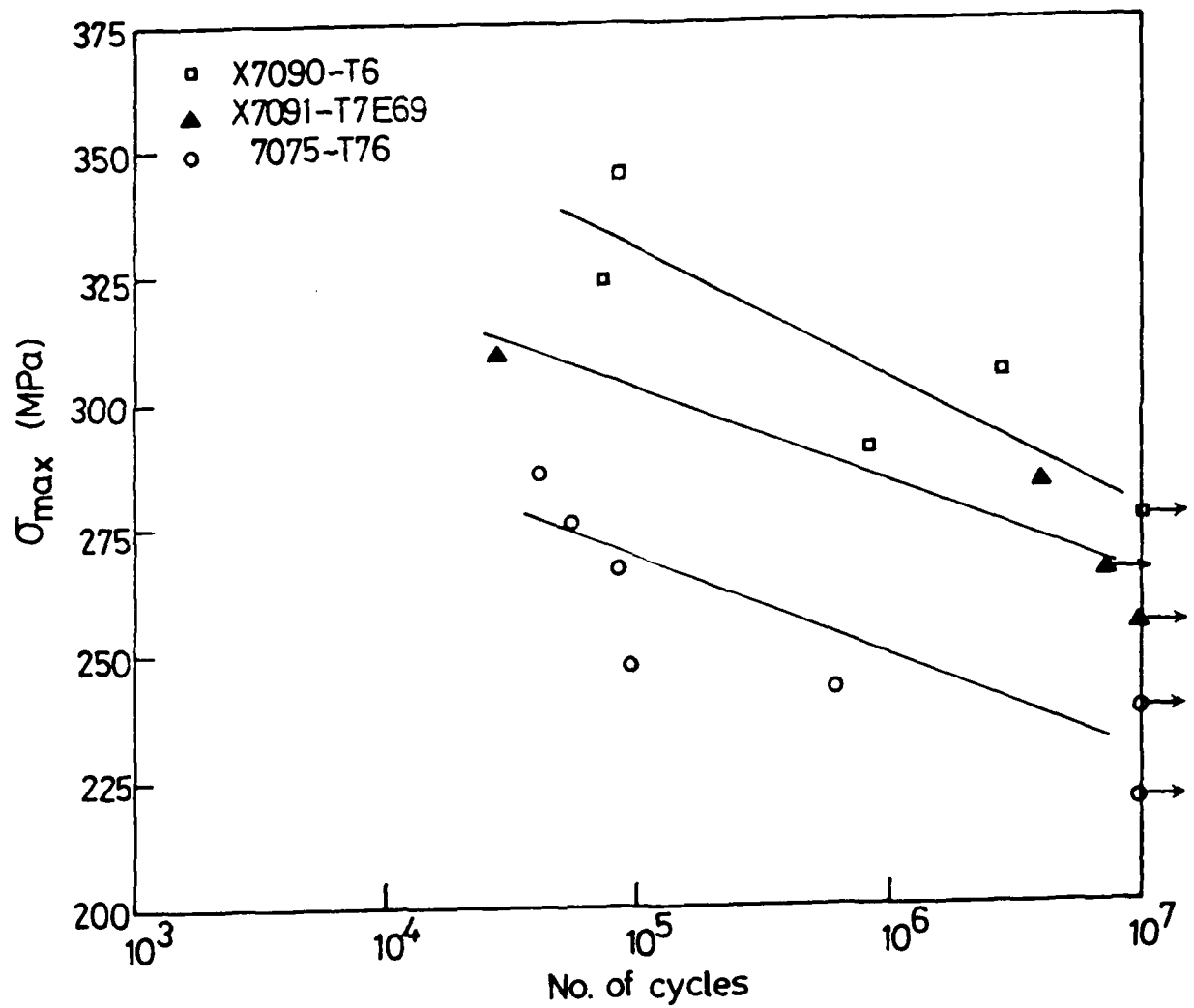

Fig. 2 Number of cycles to failure vs. maximum stress for aluminum alloys tested at $R = -1$.

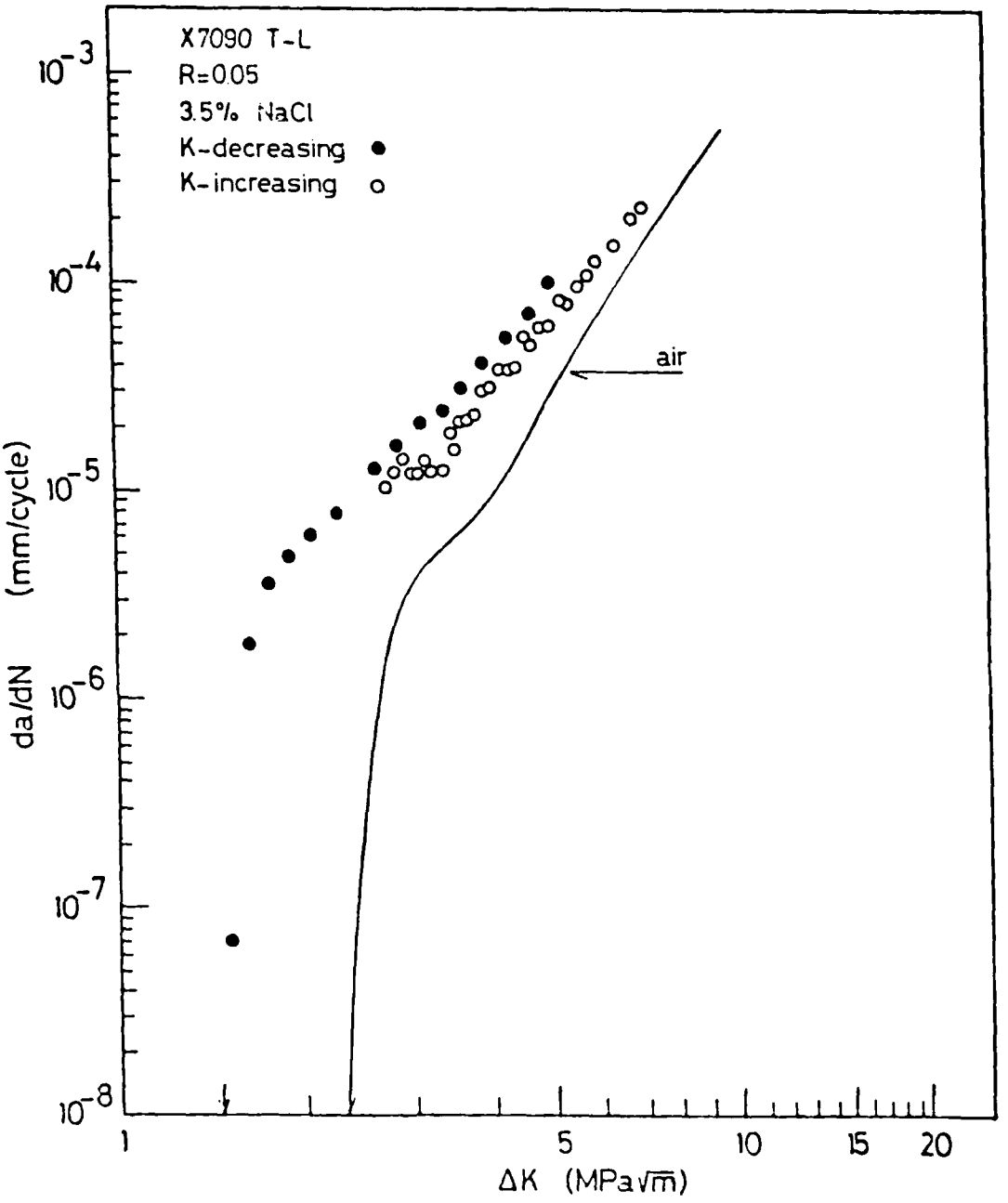

Fig. 3 Fatigue crack growth rates of X7090 aluminum alloy tested at R = 0.05 in 3.5 pct. NaCl solution.

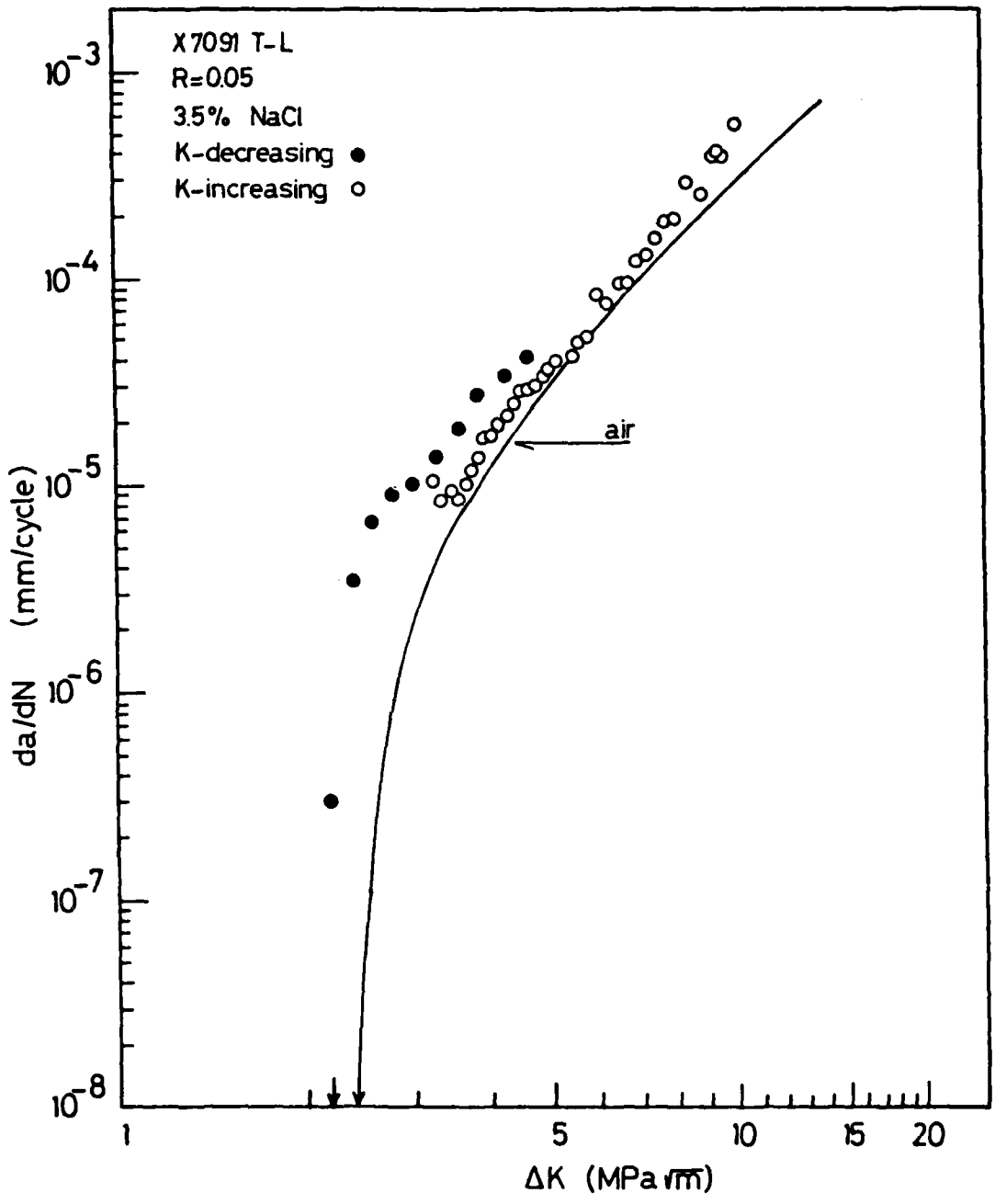

Fig. 4 Fatigue crack growth rates of X7091 aluminum alloy tested at R = 0.05 in 3.5 pct. NaCl solution.

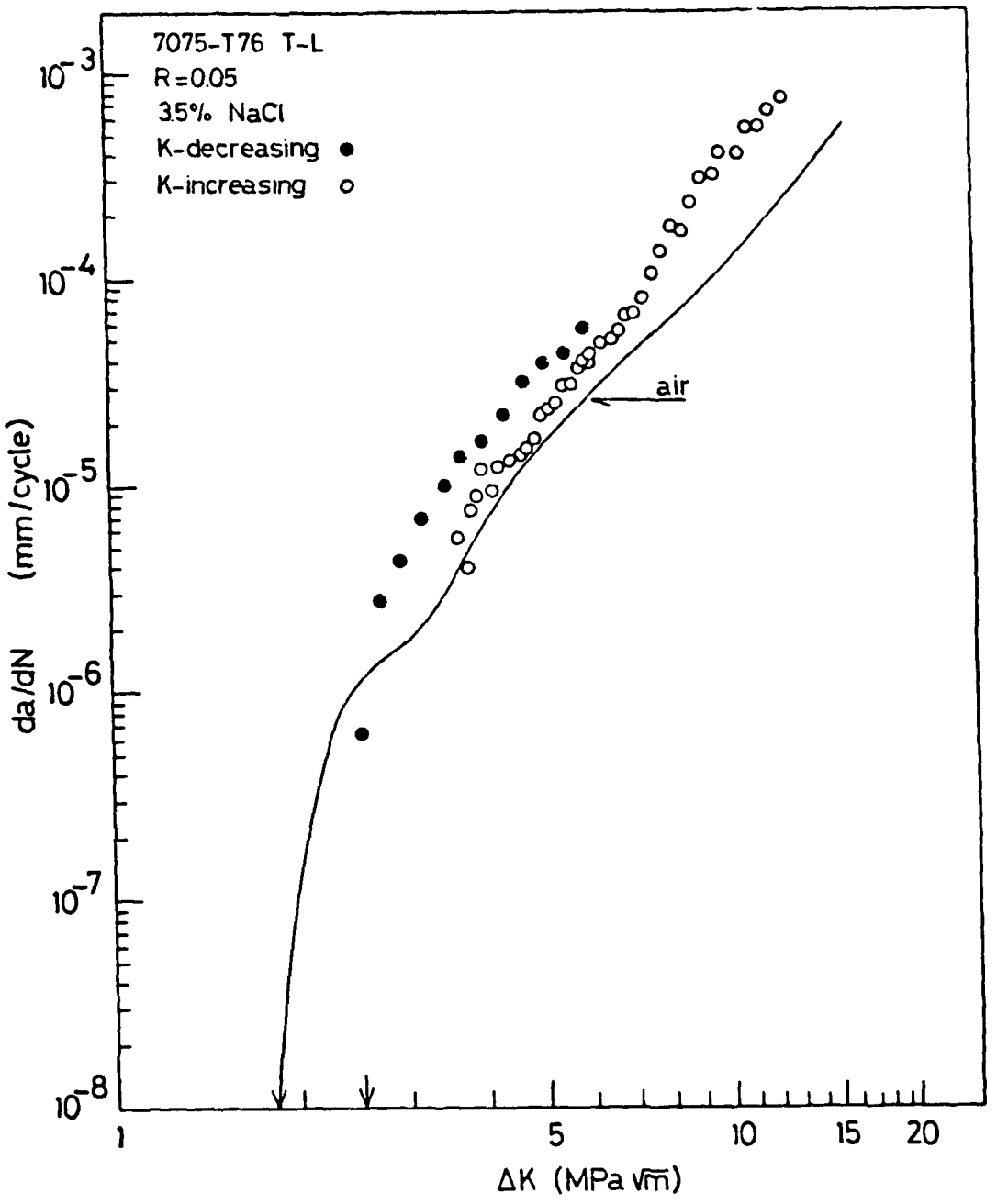

Fig. 5 Fatigue crack growth rates of 7075 aluminum alloy tested at R = 0.05 in 3.5 pct. NaCl solution.

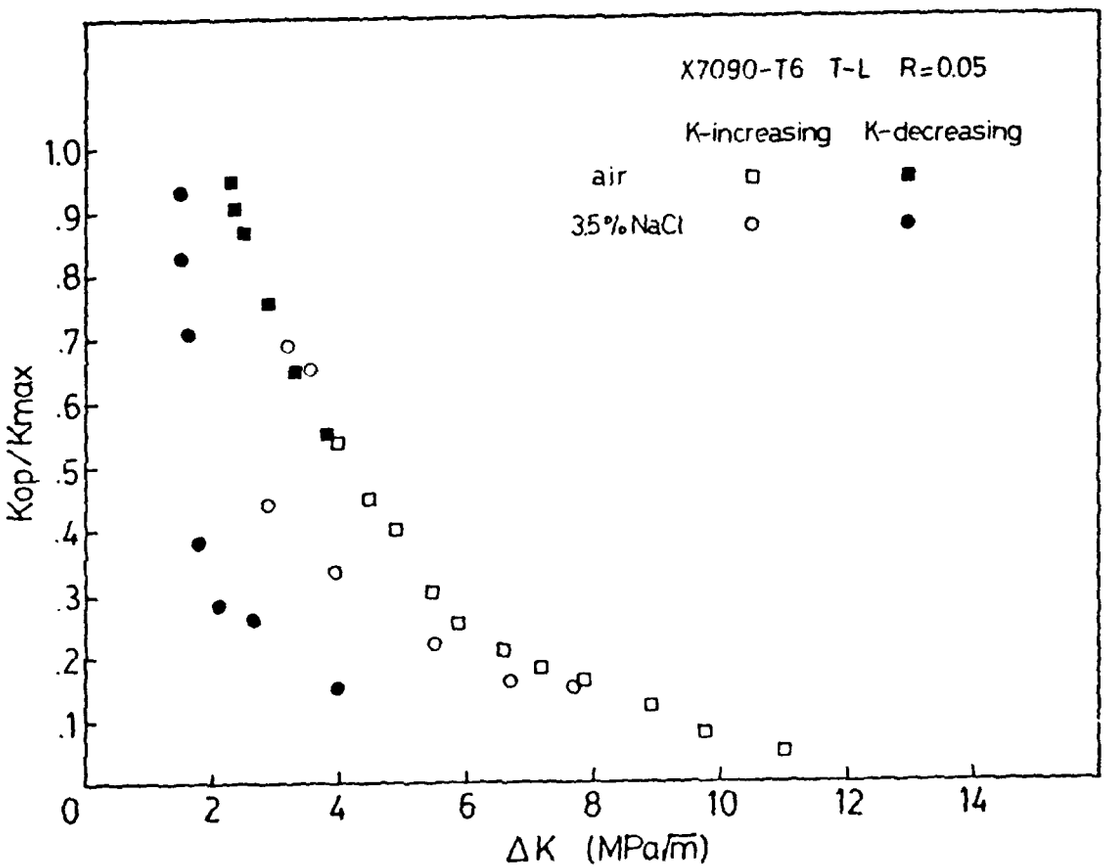

Fig. 6 Results of crack opening load measurements for X7090 aluminum alloy tested in 3.5 pct. NaCl solution.

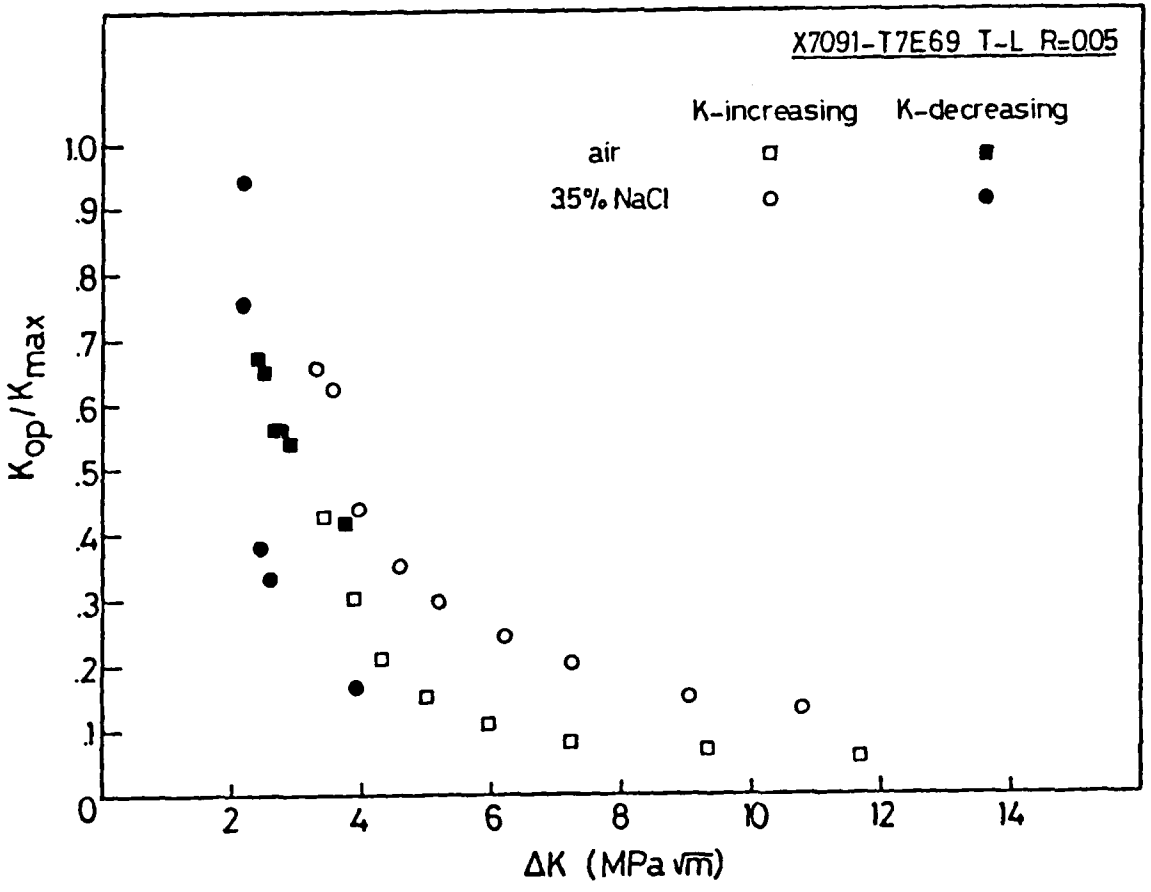

Fig. 7 Results of crack opening load measurements for X7091 aluminum alloy tested in 3.5 pct. NaCl solution.

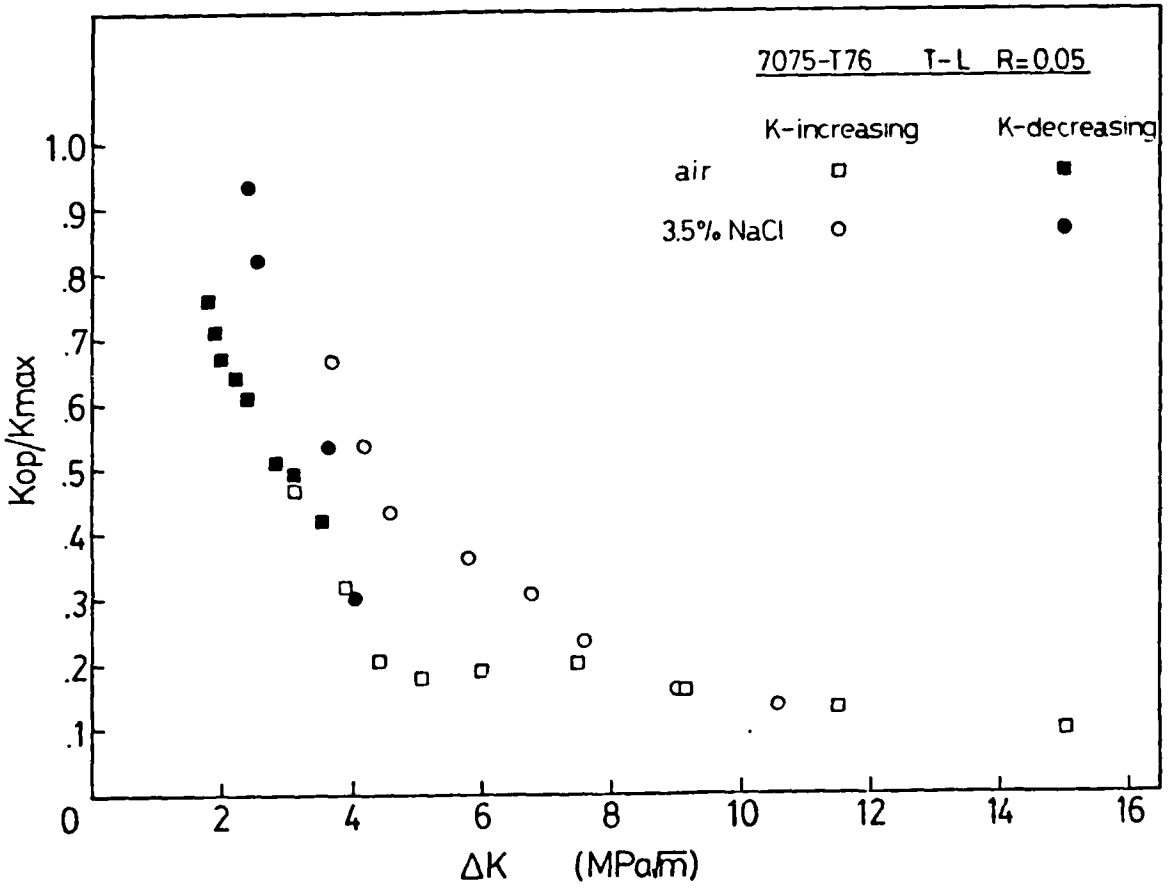

Fig. 8 Results of crack opening load measurements for 7075 aluminum alloy tested in 3.5 pct. NaCl solution.

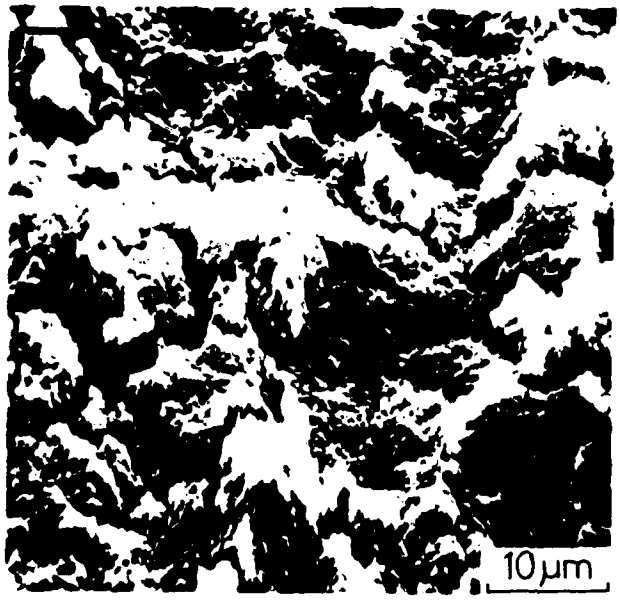

Fig. 9 Fracture surface of X7091 tested at R = 0.05 in 3.5 pct. NaCl solution. Note that corrosion products developed on the fracture surface. Arrow indicates direction of macroscopic crack growth.

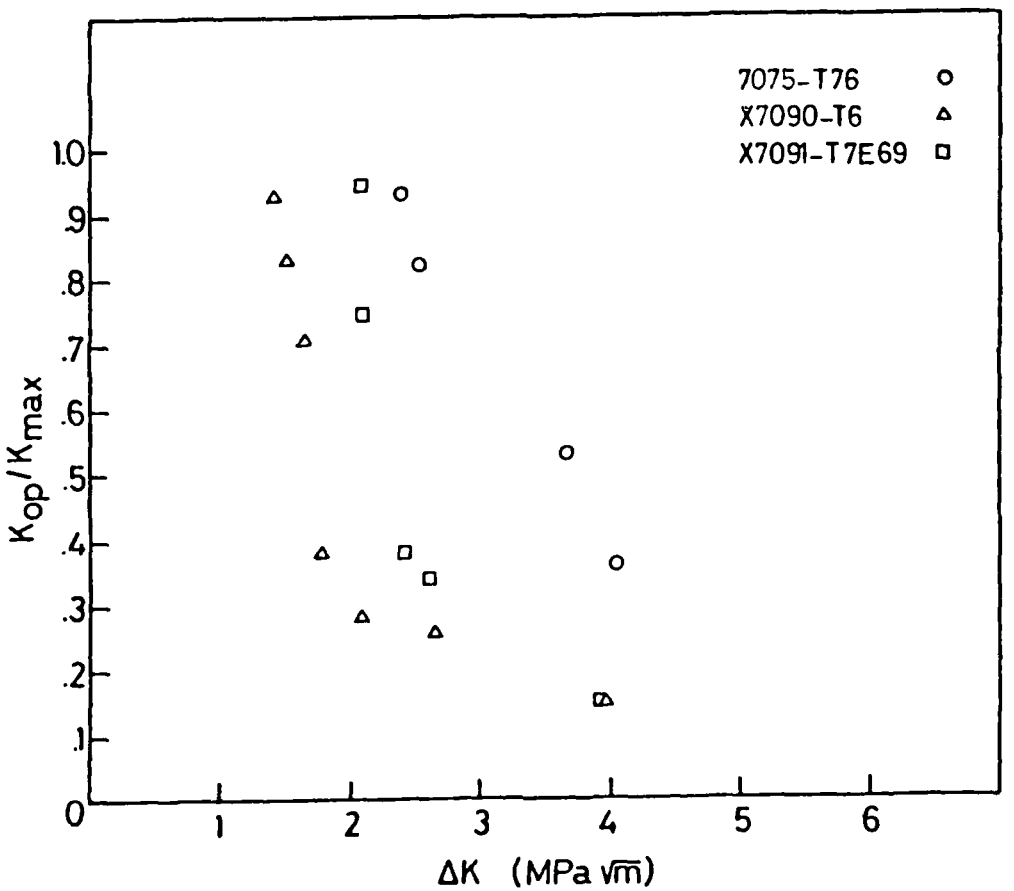

Fig. 10 Comparison of closure levels for three types of aluminum alloys tested at R = 0.05 in 3.5 pct. NaCl solution. Data points were taken from only K-decreasing tests for all alloys.

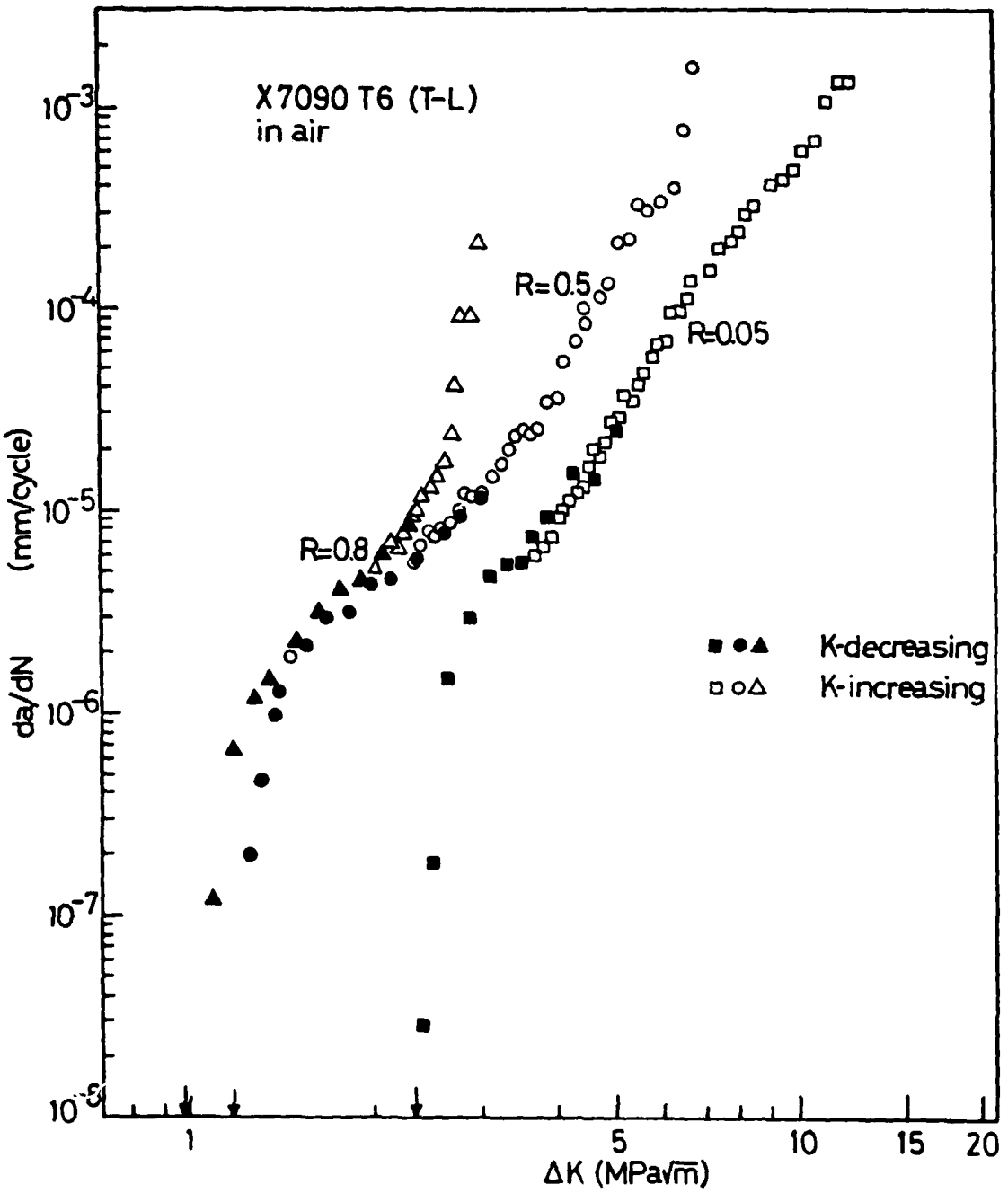

Fig. 11 Fatigue crack growth rates of X7090 aluminum alloy tested at three R ratios.

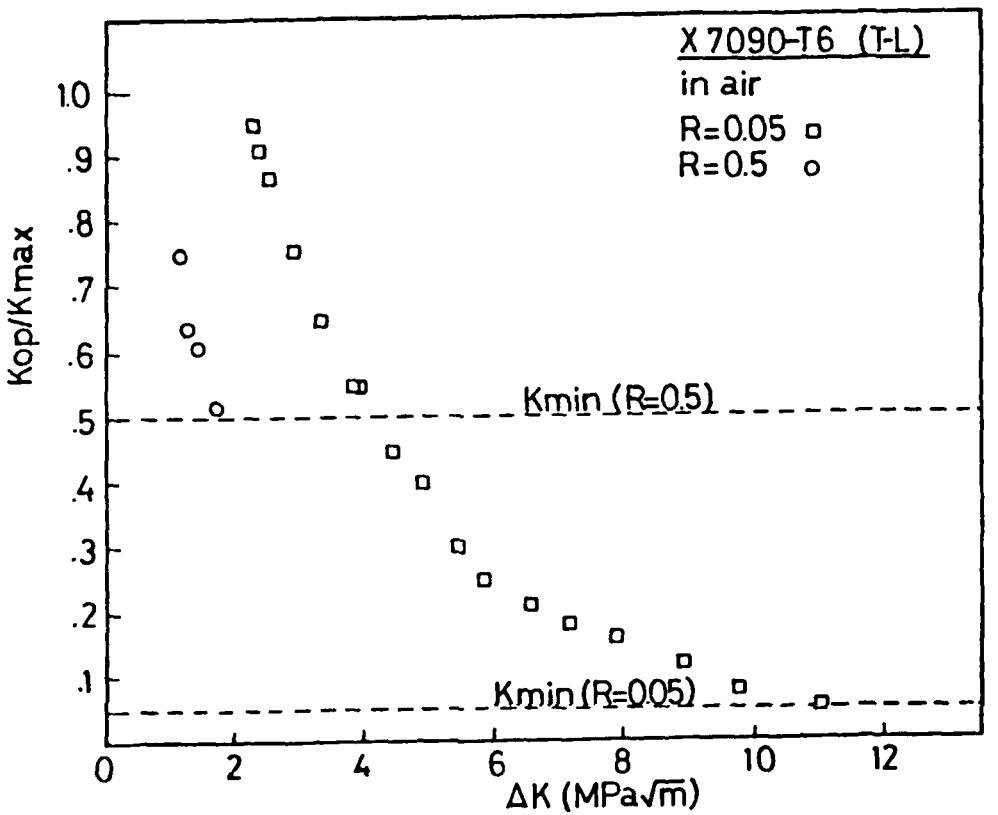

Fig. 12 Results of crack opening load measurements for X7090 aluminum alloy at three R ratios. Note that no closure was observed at R = 0.8.

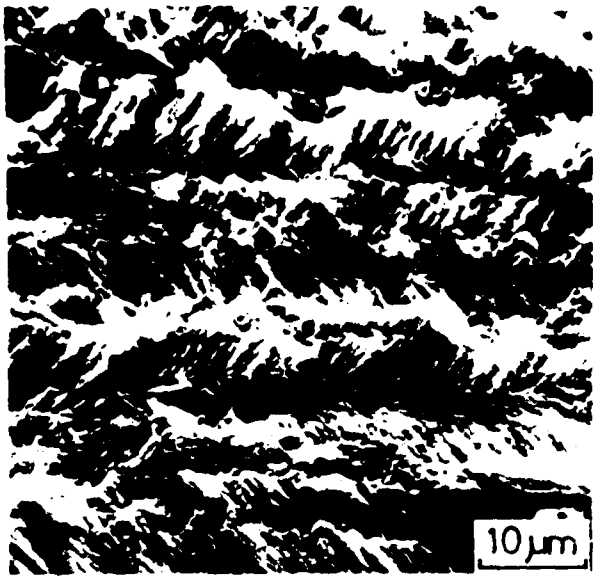

(a)

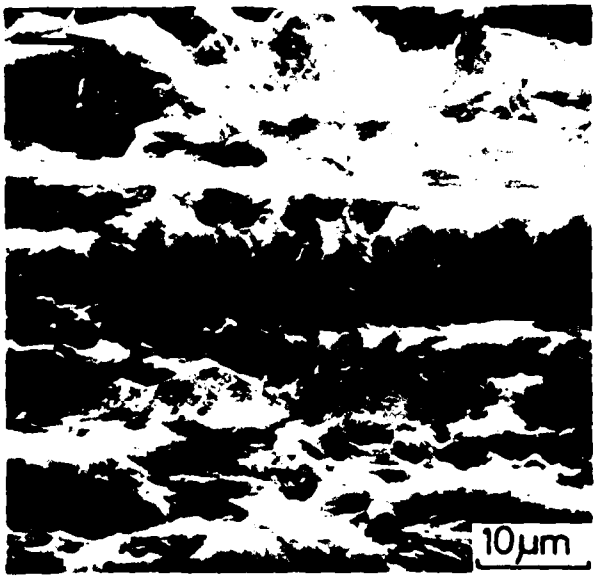

(b)

Fig. 13 Fracture surface of X7090 aluminum alloy tested at R = 0.05. Arrow indicates direction of macroscopic crack growth. (a) 5×10^{-6} m/cycle, (b) ΔK_{TH}.

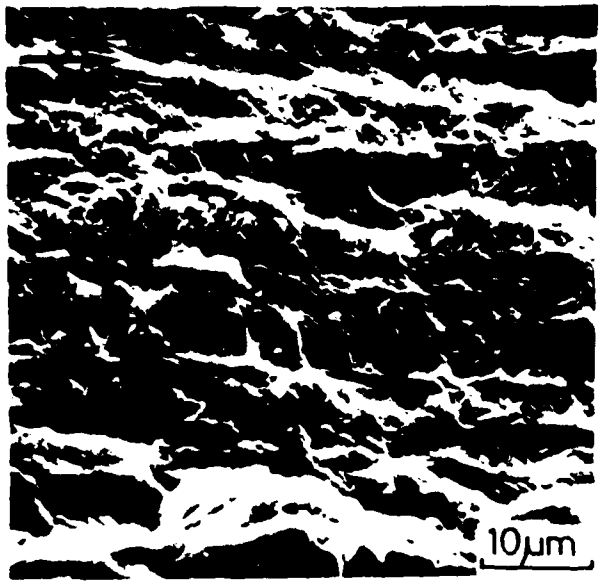

(a)

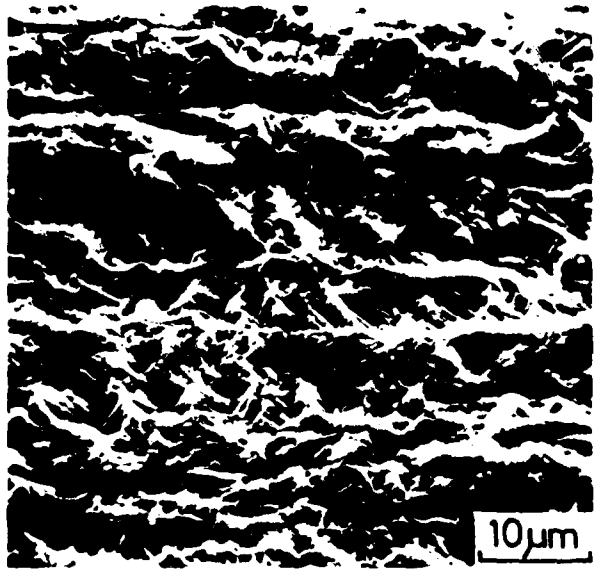

(b)

Fig. 14 Appearance of fracture surface of X7090 aluminum alloy at ΔK_{TH}. Arrow indicates direction of macroscopic crack growth. (a) R = 0.5, (b) R = 0.8.

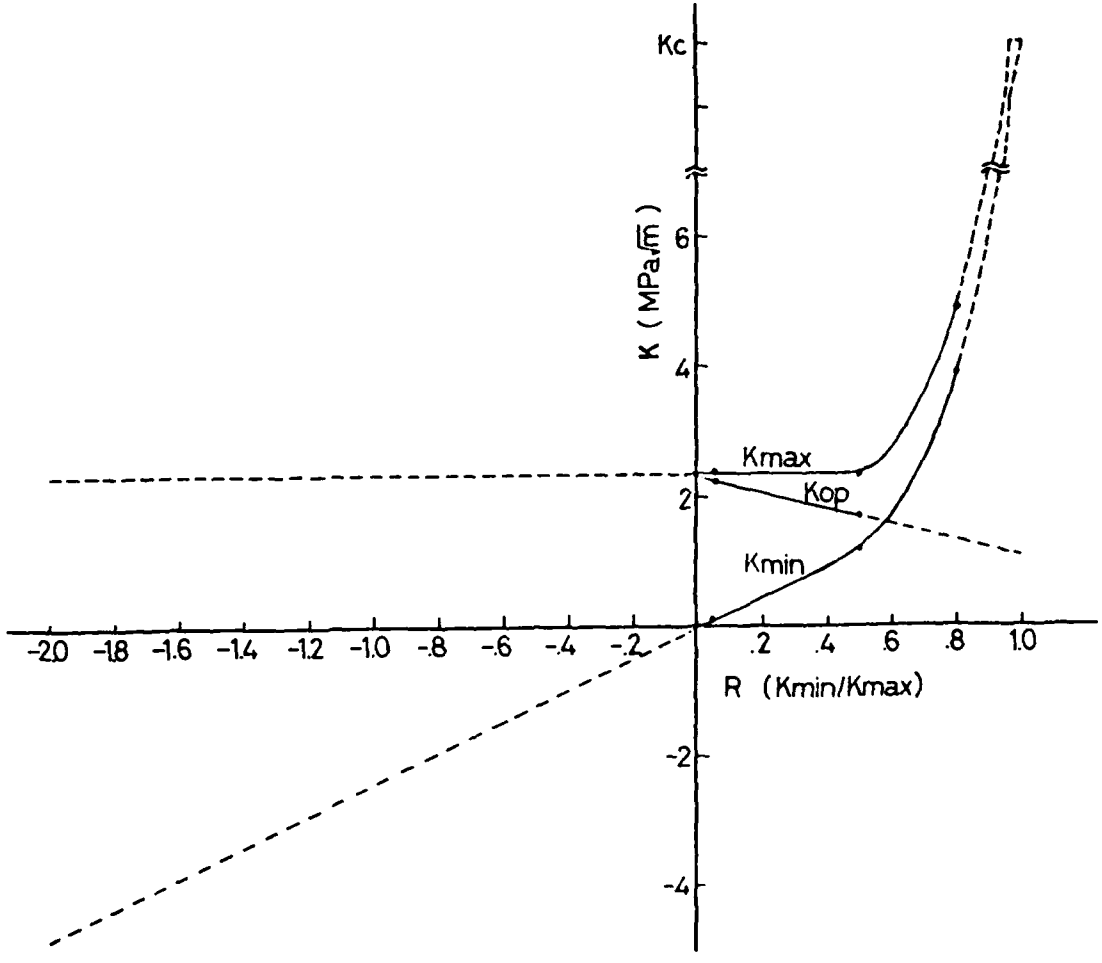

Fig. 15 Overall representation of the effect of R ratio on K_{TH}. Solid lines indicate a variation of K level obtained from the present study. Dash lines indicate an expected variation of K level as a function of R. (Assuming that a crack is fully closed at R = 0.)

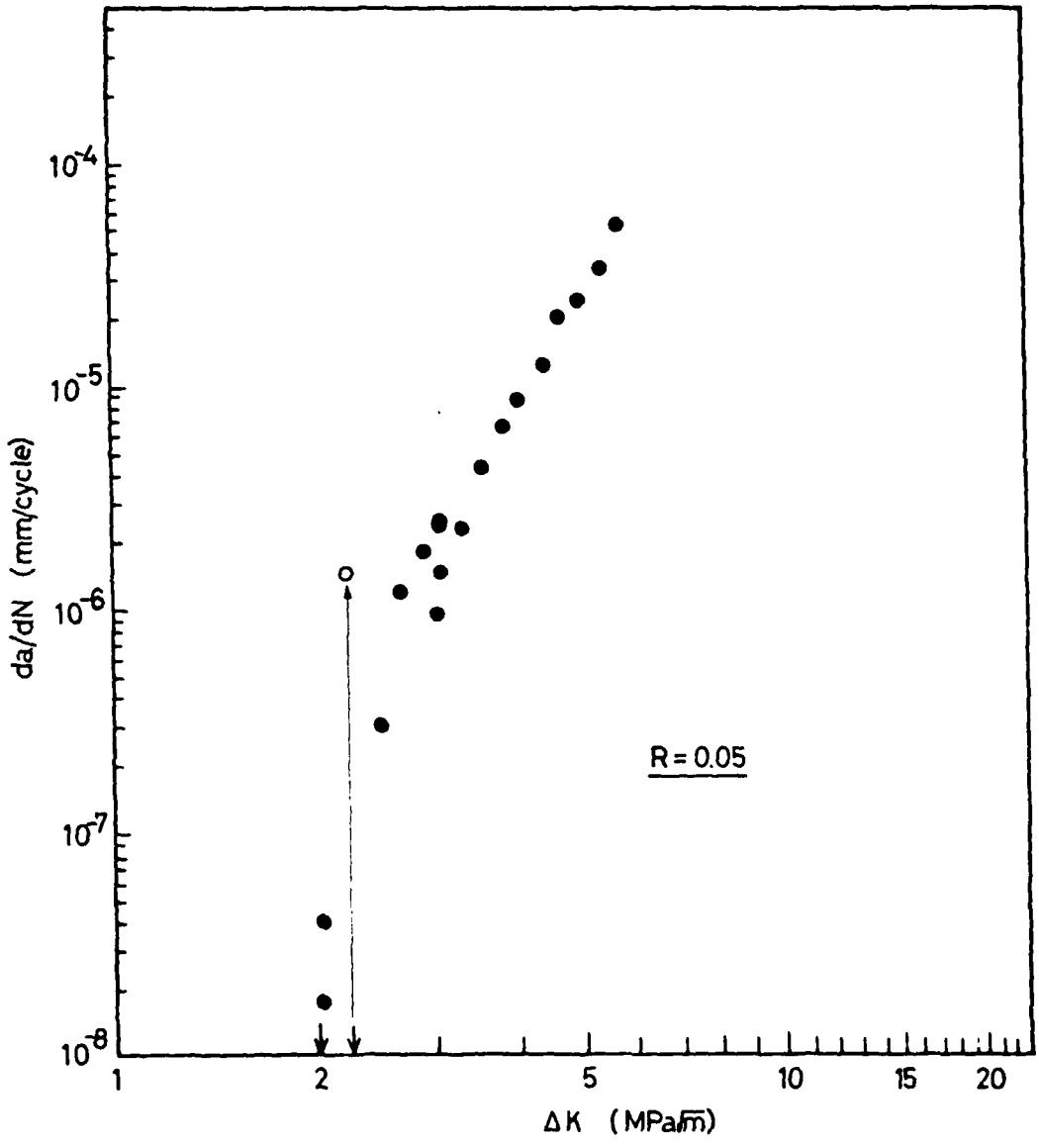

Fig. 16 Results of the near-threshold fatigue crack growth test for X7090 aluminum alloy. Note that the difference between the two thresholds is only 0.2 MPa√m.

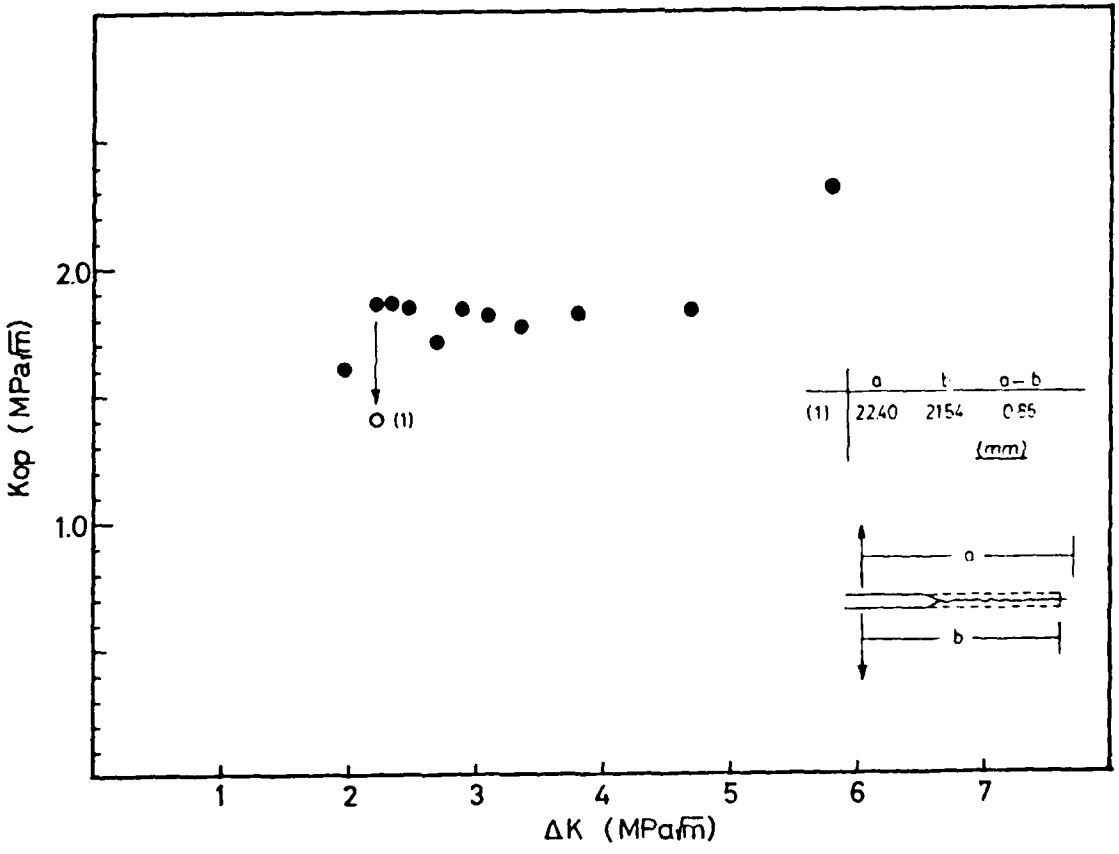

Fig. 17 Results of crack opening load measurements for X7090 aluminum alloy. Note that closure characteristics are strongly associated with the Mode II and Mode I crack growth.

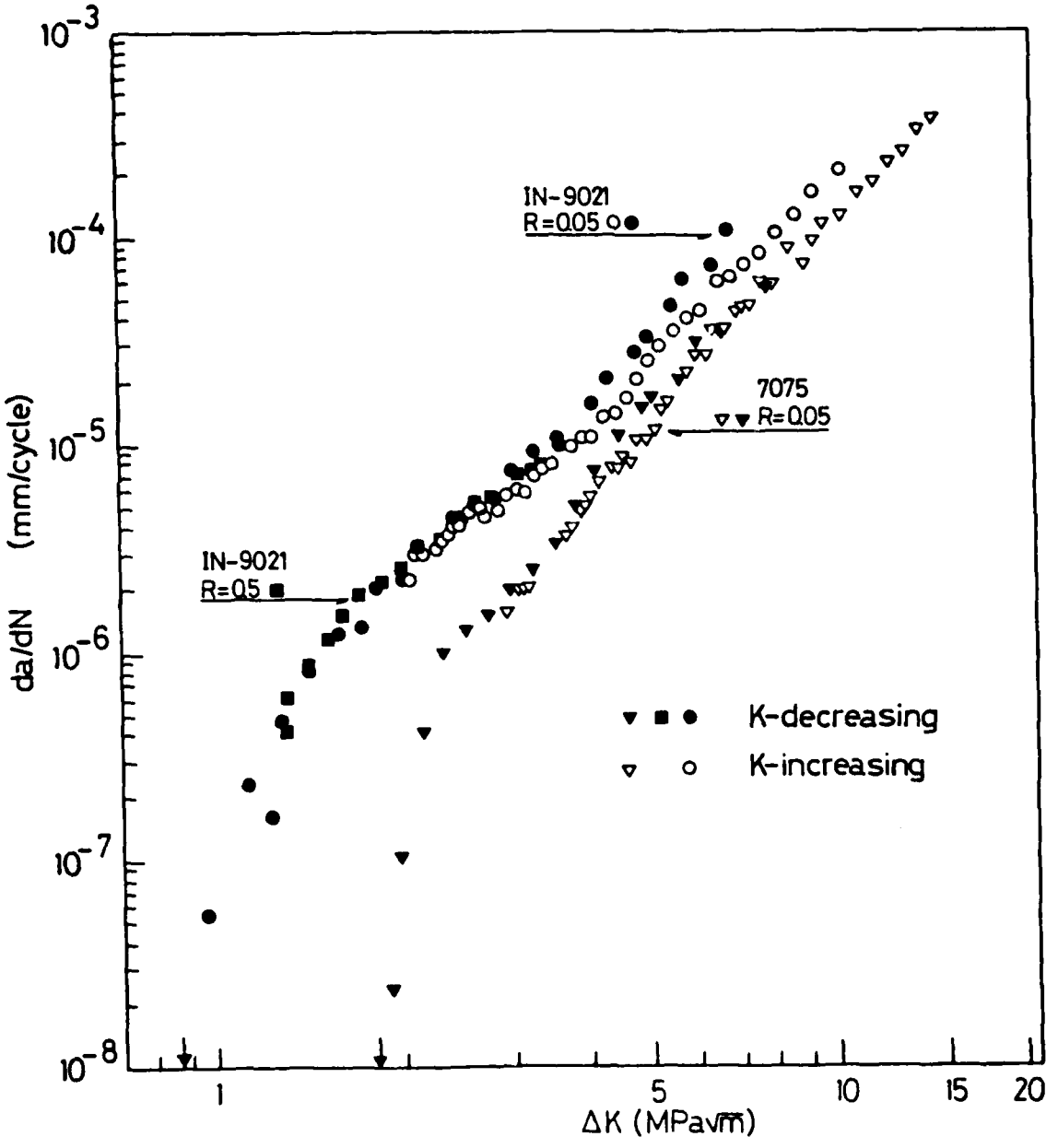

Fig. 18 Fatigue crack growth rates of IN 9021 aluminum alloy tested at R = 0.05 and R = 0.5.

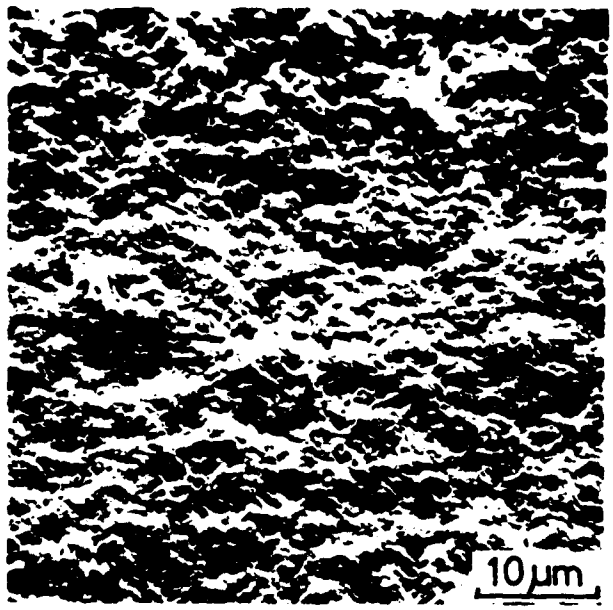

(a)

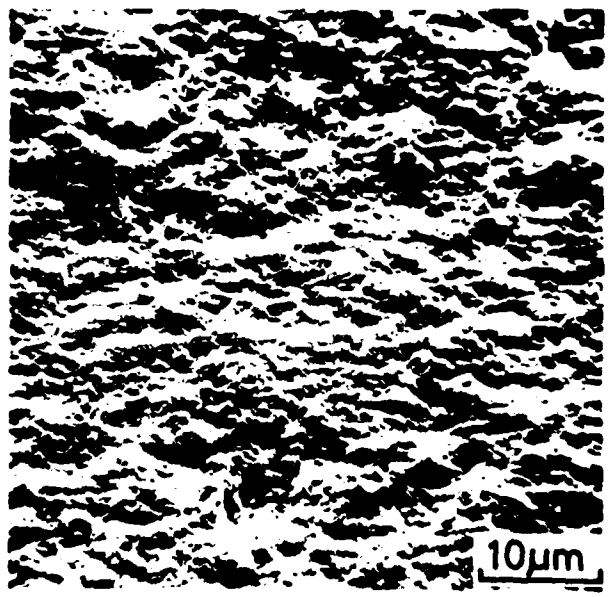

(b)

Fig. 19 Appearance of fracture surface in the near-threshold region of IN 9021 aluminum alloy tested at R = 0.05. Arrow indicates direction of macroscopic crack growth. (a) 1×10^{-6} mm/cycle, (b) ΔK_{TH}.

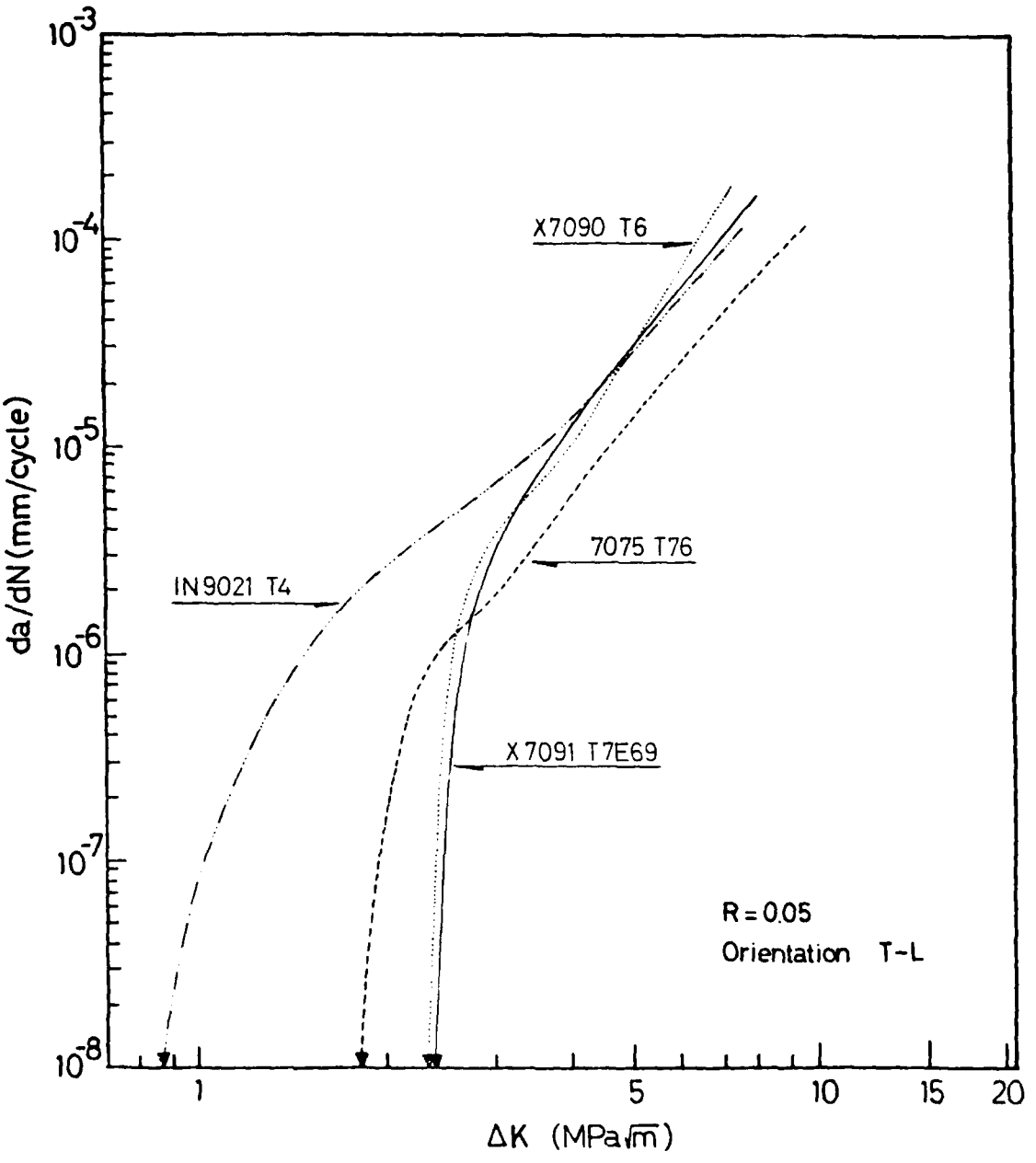

Fig. 20 Comparison of fatigue crack growth behavior in the near-threshold region for the aluminum alloys.

INSTITUTE OF MATERIALS SCIENCE

The Institute of Materials Science (IMS) was established at The University of Connecticut in 1966 in order to promote academic research programs in materials science. To provide requisite research laboratories and equipment, the State of Connecticut appropriated $5,000,000, which was augmented by over $2,000,000 in federal grants. To operate the Institute, the State Legislature appropriates over $700,000 annually for faculty and staff salaries, supplies and commodities, and supporting facilities such as an electronics shop, instrument shop, a reading room, etc. This core funding has enabled IMS to attract over $2,500,000 annually in direct grants from federal agencies and industrial sponsors.

IMS fosters interdisciplinary graduate programs in Alloy Science, Biomaterials, Corrosion Science, Crystal Science, Metallurgy, and Polymer Science. These programs are directed toward training graduate students while advancing the frontiers of knowledge and meeting current and, long-range needs of our state and our nation.

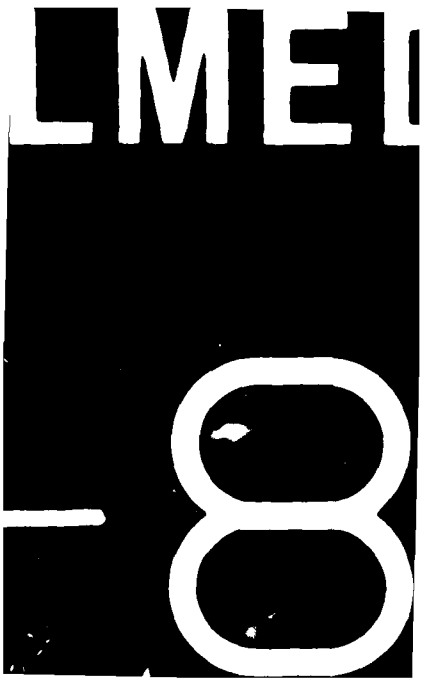
LMEL
8